New Terpyridine-Containing Macrocycle for the Assembly of Dimeric Zn(II) and Cu(II) Complexes Coupled by Bridging Hydroxide Anions and π-Stacking Interactions

11 AUTHORS, INCLUDING:

Antonio Bianchi
University of Florence
296 PUBLICATIONS **5,752** CITATIONS

Carlos Lodeiro
University NOVA of Lisbon
239 PUBLICATIONS **3,054** CITATIONS

João Carlos Lima
New University of Lisbon
143 PUBLICATIONS **2,218** CITATIONS

F. Pina
New University of Lisbon
205 PUBLICATIONS **3,789** CITATIONS

Inorganic Chemistry
Article

New Terpyridine-Containing Macrocycle for the Assembly of Dimeric Zn(II) and Cu(II) Complexes Coupled by Bridging Hydroxide Anions and π-Stacking Interactions

Carla Bazzicalupi, Andrea Bencini,* Emanuela Berni, Antonio Bianchi,* Andrea Danesi, Claudia Giorgi, and Barbara Valtancoli

Department of Chemistry, University of Florence, Via della Lastruccia 3, Sesto Fiorentino, Firenze, Italy

Carlos Lodeiro, João Carlos Lima, and Fernando Pina*

REQUIMTE - Centro de Química Fina e Biotecnologia, Departamento de Química, Faculdade de Ciências e Tecnologia, Universidade Nova de Lisboa, Quinta da Torre 2829-516 Monte de Caparica, Portugal

M. Alexandra Bernardo

REQUIMTE - Centro de Química Fina e Biotecnologia, Departamento de Química, Faculdade de Ciências e Tecnologia, Universidade Nova de Lisboa, Quinta da Torre 2829-516 Monte de Caparica, Portugal, and Instituto Superior de Ciências da Saúde-Sul, Cooperativa de Ensino Superior Egas Moniz, Campus Universitário, Quinta da Grana, 2829-511 Monte de Caparica, Portugal

The synthesis of the new terpyridine-containing macrocycle 2,5,8,11,14-pentaaza[15](6,6″)cyclo(2,2′:6′,2″)-terpyridinophane (**L**) is reported. The ligand contains a pentaamine chain linking the 6,6″ positions of a terpyridine unit. A potentiometric, ^{1}H NMR, UV–vis spectrophotometric and fluorescence emission study on the acid–base properties of **L** in aqueous solutions shows that the first four protonation steps occur on the polyamine chain, whereas the terpyridine nitrogens are involved in proton binding only at strongly acidic pH values. **L** can form both mono- and dinuclear Cu(II), Zn(II), Cd(II), and Pb(II) complexes in aqueous solution. The crystal structures of the Zn(II) and Cd(II) complexes $\{[ZnLH]_2(\mu\text{-OH})\}(ClO_4)_5$ (**6**) and $\{[CdLH]_2(\mu\text{-Br})\}(ClO_4)_5 \cdot 4H_2O$ (**7**) show that two mononuclear $[MLH]^{3+}$ units are coupled by a bridging anion (OH$^-$ in **6** and Br$^-$ in **7**) and π-stacking interactions between the terpyridine moieties. A potentiometric and spectrophotometric study shows that in the case of Cu(II) and Zn(II) the dimeric assemblies are also formed in aqueous solution containing the ligand and the metals in a 1:1 molar ratio. Protonation of the complexes or the addition of a second metal ion leads to the disruption of the dimers due to the increased electrostatic repulsions between the two monomeric units.

Introduction

There is current interest in the development of new polyamine macrocyclic receptors because of their versatile use in metal-ion chelation.[1–5] Macrocyclic polyamines containing appropriate binding sites and cavities of suitable size and shape may be designed to form selective inclusion complexes in aqueous solution. Structural factors, such as ligand rigidity and the type of donor atoms and their disposition, have been shown to play significant roles in determining the binding features of macrocycles toward metal

* Authors to whom correspondence should be addressed. Tel: 0039-055-4573371. Fax: 0039-055-4573364. E-mail: andrea.bencini@unifi.it (A.B.); fjp@dq.fct.unl.pt (F.P.).

(1) (a) Bradshaw, J. S., Krakowiak, K. E., Izatt, R. M., Eds.; *Aza-Crown Macrocycles;* Chemistry of Heterocyclic Compounds, Vol. 51; Wiley: New York, 1993. (b) Izatt, R. M.; Pawlak, K.; Bradshaw, J. S.; Bruening, R. L. *Chem. Rev.* **1995**, *95*, 2529–2586.

cations.[1-15] The resulting coordination environment of the metals strongly influences the reactivity and/or the photophysical properties of the complexes. Heteroaromatic subunits, such as 2,2′-dipyridine or 1,10-phenanthroline, are often introduced as integral parts of the host molecules.[16-23] These units are rather rigid and provide two aromatic nitrogens whose unshared electron pairs may act cooperatively in binding cations. We have found that the incorporation of these moieties into macrocyclic structures may allow them to combine within the same ligand, resulting in the special complexation features of macrocycles with the

photophysical and photochemical properties displayed by the metal complexes of these heterocycles.[20] In the course of our investigation of the cation binding capabilities of polyazamacrocycles containing heteroaromatic moieties, such as phenanthroline[21] and dipyridine,[22,23] we have synthesized the new ligand **L**, which displays a pentaamine chain linking the 6 and 6″ positions of a terpyridine unit. Both the aliphatic polyamine chain and the terpyridine moiety are potential binding sites for proton and/or metal binding. Terpyridine displays a marked binding ability for transition- and post-transition-metal cations,[24] comparable to that of an aliphatic triamine but generally lower than that of a pentaamine ligand. At the same time, this heteroaromatic unit shows a lower affinity for acidic protons than aliphatic amines. Because the process of metal coordination in aqueous solution is competitive with proton binding, the coordination properties of this ligand would be, in principle, modulated by a subtle balance of the different affinity of the heteroaromatic unit and the polyamine chain toward acidic protons and metal

(2) Lehn, J.-M. *Supramolecular Chemistry: Concepts and Perspectives;* VCH: New York, 1995.

(3) (a) Lindoy, L. F. *The Chemistry of Macrocyclic Ligand Complexes*; Cambridge University Press: Cambridge, U.K., 1992. (b) Lindoy, L. F. *Pure Appl. Chem.* **1997**, *69*, 2179−2184.

(4) (a) Raidt, R.; Neuburger, M.; Kaden, T. A. *Dalton Trans.* **2003**, 1292− 1298. (b) Kaden, T. A. *Coord. Chem. Rev.* **1999**, *190−192*, 371− 389.

(5) Blake, A. J.; Champness, N. R.; Hubberstey, P.; Li, W. S.; Schröder, M.; Withersby, M. A. *Coord. Chem. Rev.* **1999**, *183*, 117−138.

(6) Nelson, J.; McKee, V.; Morgan, G. *Prog. Inorg. Chem.* **1998**, *47*, 167− 316.

(7) (a) Katrintzky, A. R., Rees, C. W., Schriven, E., Eds.; *Comprehensive Coordination Chemistry*; Pergamon: Oxford, U.K., 1996; Vol. 9. (b) Bencini, A.; Bianchi, A.; Paoletti, P.; Paoli, P. *Coord. Chem. Rev.* **1992**, *120*, 51−85.

(8) (a) Fry, F. H.; Fallon, G. D.; Spiccia, L. *Inorg. Chim. Acta* **2003**, *346*, 57−66. (b) Fry, F. H.; Jensen, P.; Kepert, C. M.; Spiccia, L. *Inorg. Chem.* **2003**, *42*, 5637−5644. (c) Fry, F. H.; Moubaraki, B.; Murray, K. S.; Spiccia, L.; Warren, M.; Skelton, B. W.; White, A. H. *J. Chem. Soc., Dalton Trans.* **2003**, 866−871. (d) Brudenell, J. S.; Spiccia, L.; Hockless, D. C. R.; Tiekink, E. R. T. *J. Chem. Soc., Dalton Trans.* **1999**, 1475−1482.

(9) Ghosh, P.; Bharadwaj, P. K.; Roy, J.; Ghosh, S. *J. Am. Chem. Soc.* **1997**, *119*, 11903−11909.

(10) (a) Depree, C. V.; Beckmann, U.; Heslop, K.; Brooker, S. *J. Chem. Soc., Dalton Trans.* **2003**, 3071−3081. (b) Brooker, S. *Coord. Chem. Rev.* **2001**, *222*, 33−56.

(11) (a) Lamarque, L.; Miranda, C.; Navarro, P.; Escartí, F.; García-España,E.; LaTorre, J.; Ramírez, J. A. *Chem. Commun.* **2000**, 1337− 1338. (b) Lamarque, L.; Navarro, P.; Miranda, C.; Aran, V. J.; Ochoa, C.; Escartí, F.; García-España, E.; LaTorre, J.; Luis, S. V.; Miravet, J. F. *J. Am. Chem. Soc.* **2001**, *123*, 10560−10570.

(12) (a) Ambrosi, G.; Dapporto, P.; Formica, M.; Fusi, V.; Giorgi, L.; Guerri, A.; Micheloni, M.; Paoli, P.; Pontellini, R.; Rossi, P. *Chem.− Eur. J.* **2003**, *9*, 800−810. (b) Dapporto, P.; Formica, M.; Fusi, V.; Giorgi, L.; Micheloni, M.; Paoli, P.; Pontellini, R.; Rossi, P. *Inorg. Chem.* **2001**, *40*, 6186−6192.

(13) Guerriero, P.; Tamburini, S.; Vigato, P. A. *Coord. Chem. Rev.* **1995**, *139*, 17−243.

(14) Izatt, R. M.; Pawlak, K.; Bradshaw, J. S.; Bruenig, R. L. *Chem. Rev.* **1991**, *91*, 1721−1985.

(15) (a) Fabbrizzi, L.; Licchelli, M.; Rabaioli, G.; Taglietti, A. *Coord. Chem. Rev.* **2000**, *205*, 85−108. (b) Fabbrizzi, L.; Licchelli, M.; Pallavicini, P. *Acc. Chem. Res.* **1999**, *32*, 846−853. (c) Fabbrizzi, L.; Licchelli, M.; Taglietti, A. *J. Chem. Soc., Dalton Trans.* **2003**, 3471−3479. (d) Amendola, V.; Fabbrizzi, L.; Mangano, C.; Pallavicini, P. *Struct. Bonding (Berlin)* **2001**, *99*, 79−115 (e) Hortala, M. A.; Fabbrizzi, L.; Marcotte, N.; Stomeo, F.; Taglietti, A. *J. Am. Chem. Soc.* **2003**, *125*, 20−21.

(16) (a) Blake, A. J.; Demartin, F.; Devillanova, F. A.; Garau, A.; Isaia, F.; Lippolis, V.; Schröder, M.; Verani, G. *J. Chem. Soc., Dalton Trans.* **1996**, 3705−3712. (b) Blake, A. J.; Casabo, J.; Devillanova, F. A.; Escriche, L.; Garau, A.; Isaia, F.; Lippolis, V.; Kivekas, R.; Muns, V.; Schröder, M.; Sillampää, R.; Verani, G. *J. Chem. Soc., Dalton Trans.* **1999**, 1085−1092. (c) Arca, M.; Blake, A. J.; Casabo, J.; Demartin, F.; Devillanova, F. A.; Garau, A.; Isaia, F.; Lippolis, V.; Kivekas, R.; Muns, V.; Schröder, M.; Verani, G.; *J. Chem. Soc., Dalton Trans.* **2001**, 1180−1188.

(17) (a) Azéma, J.; Galaup, C.; Picard, C.; Tisnès, P.; Ramos, P.; Juanes, O.; Rodrìguez-Ubis, J. C.; Brunet, E. *Tetrahedron* **2000**, *56*, 2673− 2681 and references therein. (b) Galaup, C.; Carrié, M.-C.; Tisnès, P.; Picard, C. *Eur. J. Org. Chem.* **2001**, 2165−2175. (c) Galaup, C.; Couchet, J. M.; Picard, C.; Tisnès, P. *Tetrahedron Lett.* **2001**, *42*, 6275−6278.

(18) (a) Rodriguez-Ubis, J.-C.; Alpha, B.; Plancherel, D.; Lehn, J. M. *Helv. Chim. Acta* **1984**, *67*, 2264−2269. (b) Alpha, B.; Lehn, J. M.; Mathis, G. *Angew. Chem., Int. Ed. Engl.* **1987**, *99*, 259−261. (c) Cesario, M.; Guilhem, J.; Pascard, C.; Anklam, E.; Lehn, J. M.; Pietraskiewicz, M. *Helv. Chim. Acta* **1991**, *74*, 1157−1162. (d) Bkouche-Waksmann, I.; Guilhem, J.; Pascard, C.; Alpha, B.; Deschenaux, Lehn, J. M. *Helv. Chim. Acta* **1991**, *75*, 1163−1170. (e) Lehn, J. M.; Regnouf de Vains, J. B. *Helv. Chim. Acta* **1992**, *75*, 1221−1236. (f) Paul-Roth, C. O.; Lehn, J.-M.; Guilheim, J.; Pascard, C. *Helv. Chim. Acta* **1995**, *78*, 1895−1903 and references therein.

(19) (a) Vidal, P.-L.; Divisia-Blohorn, B.; Bidan, G.; Kern, J.-M.; Sauvage, J.-P.; Hazemann, J.-L. *Inorg Chem.* **1999**, *38*, 4203−4210. (b) Weck, M.; Mohr, B.; Sauvage, J.-P.; Grubbs, R. H. *J. Org. Chem.* **1999**, *64*, 5463−5471. (c) Rapenne, G.; Dietrich-Buchecker, C.; Sauvage, J.-P. *J. Am. Chem. Soc.* **1999**, *121*, 994−1001. (d) Meyer, M.; Albrecht-Gary, A.-M.; Dietrich-Buchecker, C. O.; Sauvage, J.-P. *Inorg. Chem.* **1999**, *38*, 2279−2287.

(20) (a) Barigelletti, F.; De Cola, L.; Balzani, V.; Belser, P.; Von Zelewsky, A.; Vögtle, F.; Ebmeyer, F.; Grammenudi, S. *J. Am. Chem. Soc.* **1989**, *111*, 4662−4668. (b) Balzani, V.; Ballardini, R.; Bolletta, F.; Gandolfi, M. T.; Juris, A.; Maestri, M.; Manfrin, M. F.; Moggi, L.; Sabbatini, N. *Coord. Chem. Rev.* **1993**, *125*, 75−88 and references therein. (c) Sabbatini, N.; Guardigli, M.; Lehn, J.-M. *Coord. Chem. Rev.* **1993**, *123*, 201−228. (d) Balzani, V.; Credi, A.; Venturi, M. *Coord. Chem. Rev.* **1998**, *171*, 3−16 and references therein.

(21) (a) Bazzicalupi, C.; Bencini, A.; Fusi, V.; Giorgi, C.; Paoletti, P.; Valtancoli, B. *Inorg. Chem.* **1998**, *37*, 941−948. (b) Bazzicalupi, C.; Bencini, A.; Fusi, V.; Giorgi C.; Paoletti, P.; Valtancoli, B. *J. Chem. Soc., Dalton Trans.* **1999**, 393−400. (c) Bazzicalupi, C.; Bencini, A.; Bianchi, A.; Giorgi, C.; Fusi, V.; Valtancoli, B.; Bernardo, M. A.; Pina, F. *Inorg. Chem.* **1999**, *38*, 3806−3813. (d) Bazzicalupi, C.; Beconcini, A.; Bencini, A.; Giorgi, C.; Fusi, V.; Masotti, A.; Valtancoli, B. *J. Chem. Soc., Perkin Trans. 2* **1999**, 1675−1682. (e) Bencini, A.; Bernardo, M. A.; Bianchi, A.; Fusi, V.; Giorgi, C.; Pina, F.; Valtancoli, B. *Eur. J. Inorg. Chem.* **1999**, 1911−1918.

(22) (a) Bazzicalupi, C.; Bencini, A.; Ciattini, S.; Giorgi, C.; Masotti, A.; Paoletti, P.; Valtancoli, B.; Navon, N.; Meyerstein, D. *J. Chem. Soc., Dalton Trans.* **2000**, 2383−2391. (b) Bazzicalupi, C.; Bencini, A.; Bianchi, A.; Giorgi, C.; Fusi, V.; Masotti, A.; Valtancoli, B.; Roque, A.; Pina, F. *Chem. Commun.* **2000**, 561−562. (c) Bencini, A.; Bianchi, A.; Lodeiro, C.; Masotti, A.; Parola, A. J.; Melo, J. S.; Pina, F.; Valtancoli, B. *Chem. Commun.* **2000**, 1639−1640. (d) Bencini, A.; Bianchi, A.; Fusi, V.; Giorgi, C.; Masotti, A.; Paoletti, P. *J. Org. Chem.* **2000**, *65*, 7686−7689. (e) Bazzicalupi, C.; Bencini, A.; Berni, E.; Bianchi, A.; Giorgi, C.; Fusi, V.; Valtancoli, B.; Lodeiro, C.; Roque, A.; Pina, F. *Inorg. Chem.* **2001**, *40*, 6172−6179.

(23) (a) Lodeiro, C.; Parola, A. J.; Pina, F.; Bazzicalupi, C.; Bencini, A.; Bianchi, A.; Giorgi, C.; Masotti, A.; Valtancoli, B. *Inorg. Chem.* **2001**, *40*, 2968−2975. (b) Arranz, P.; Bazzicalupi, C.; Bencini, A.; Bianchi, A.; Ciattini, S.; Fornasari, P.; Giorgi, C.; Valtancoli, B. *Inorg. Chem.* **2001**, *40*, 6383−6389.

(24) Smith, R. M.; Martell, A. E. *NIST Stability Constants Database*, version 4.0; National Institute of Standards and Technology: Washington, DC, 1997.

ions. We decided, therefore, to carry out a study of the binding properties of **L**

L
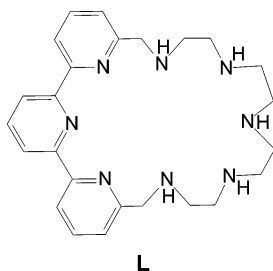
in aqueous solutions toward protons and Cu(II), Zn(II), Cd(II), and Pb(II), and the results are herein reported.

Experimental Section

1,4,7,10,13-Pentatosyl-1,4,7,10,13-pentaazatridecane (**1**)[25] and 6,6″-bis(bromomethyl)-[2,2′:6′,2″]terpyridine[17c,26] (**2**) were prepared as previously described. We recorded 300.0-MHz ^{1}H and 75.4-MHz ^{13}C NMR spectra in D_2O or $CDCl_3$ solutions at 298 K on a Varian Gemini spectrometer. In ^{1}H NMR spectra, peak positions are reported relative to TMS ($CDCl_3$ solutions) or to HOD at 4.79 ppm (D_2O solutions). Dioxane was used as the reference standard in ^{13}C NMR spectra ($\delta = 67.2$ ppm) in D_2O solutions. UV–vis absorption spectra were recorded on a Perkin-Elmer Lambda 9 spectrophotometer. HCl and NaOH were used to adjust the pH values, which were measured on a Metrohm 713 pH meter. Fluorescence emission spectra were recorded on a Horiba-Jobin Yvon-Spex Fluorolog 3.22 spectrofluorimeter equipped with a ThermoNeslab RTE7 bath. Calculations were performed using the Hyperchem software package.[27] Zindo-S calculations (RHF level) with interaction of 99 single excited configurations were performed on geometries optimized with MM+.

Synthesis of the Ligands and Their Metal Complexes. 2,5,8,-11,14-Pentatosyl-2,5,8,11,14-pentaaza[15](6,6″)cyclo(2,2′:6′,2″)-terpyridinophane (3) and 2,5,8,11,14,32,35,38,41,44-Decatosyl-2,5,8,11,14,32,35,38,41,44-decaaza[30](6,6″)cyclo(2,2′:6′,2″)bis-terpyridinophane (4). A suspension of 6,6″-bis(bromomethyl)-[2,2′:6′,2″]terpyridine (**2**) (1.05 g, 2.50 mmol) in dry CH_3CN (250 cm³) was added dropwise over a period of 4 h to a refluxing and vigorously stirred suspension of **1** (2.40 g, 2.50 mmol) and K_2CO_3 (3.46 g, 25.0 mmol) in dry CH_3CN (250 cm³). After the addition was completed, the solution was refluxed for an additional 5 h. The resulting suspension was filtered through Celite, and the solution was vacuum evaporated to give a crude oil, which was purified by column chromatography on neutral alumina (2.5 activity) (CH_2Cl_2/ethyl acetate, 10:1 v/v). The eluted fractions containing **3** ($R_f = 0.58$ CH_2Cl_2/ethyl acetate, 20:1 v/v) and **4** ($R_f = 0.44$ CH_2-Cl_2/ethyl acetate, 20:1 v/v) were collected separately and evaporated to dryness, affording **3** and **4** as white solid compounds.

3: Yield: 1.73 g (1.42 mmol, 57%). ^{1}H NMR ($CDCl_3$): δ 8.33 (d, $J = 7.97$ Hz, 2H), 8.11 (d, $J = 7.97$ Hz, 2H), 7.88 (t, $J = 7.97$ Hz, 2H), 7.80 (d, $J = 8.24$ Hz, 4H), 7.74 (t, $J = 7.97$ Hz, 1H), 7.62 (d, $J = 8.24$ Hz, 4H), 7.46 (d, $J = 7.97$ Hz, 2H), 7.38 (d, $J = 8.24$ Hz, 4H), 7.29 (d, $J = 7.97$ Hz, 2H), 7.28 (d, $J = 8.24$ Hz, 4H), 7.07 (d, $J = 7.97$ Hz, 2H), 4.44 (br s, 4H), 3.48−3.32 (m, 4H), 3.10−2.92 (m, 4H), 2.53 (br s, 8H), 2.47 (s, 6H), 2.43 (s,

(25) Bencini, A.; Bianchi, A.; García-España, E.; Giusti, M.; Micheloni, M.; Paoletti, P. *Inorg. Chem.* **1987**, *26*, 681−686.
(26) Offermann, W.; Vögtle, F. *Synthesis* **1977**, 272−273.
(27) Hyperchem, release 6.01 for Windows; Hypercube, Inc.: Gainsville, FL, 2000.

6H), 2.35 (s, 3H). ^{13}C NMR ($CDCl_3$): δ 155.6, 155.4, 154.9, 143.5, 143.4, 143.1, 138.2, 137.5, 135.4, 135.2, 135.0, 129.8, 129.6, 129.4, 127.1, 127.3, 126.9, 124.1, 121.3, 121.1, 54.7, 48.3, 48.1, 47.8, 46.1, 21.7, 21.5, 21.4. Anal. Calcd. for $C_{60}H_{64}N_8S_5O_{10}$: C, 59.19; H, 5.30; N, 9.20. Found: C, 59.5; H, 5.4; N, 9.1.

4: Yield: 0.52 g (0.21 mmol, 17%). ^{1}H NMR ($CDCl_3$): δ 8.48 (d, $J = 7.69$ Hz, 4H), 8.05 (d, $J = 7.69$ Hz, 4H), 7.79 (t, $J = 7.69$ Hz, 4H), 7.72 (d, $J = 8.24$ Hz, 4H), 7.68 (d, $J = 8.24$ Hz, 8H), 7.60 (t, $J = 7.69$ Hz, 2H), 7.46 (d, $J = 8.24$ Hz, 8H), 7.37 (d, $J = 7.69$ Hz, 4H), 7.24 (d, $J = 8.24$ Hz, 4H), 7.10 (d, $J = 8.24$ Hz, 8H), 7.03 (d, $J = 8.24$ Hz, 8H), 4.60 (br s, 8H), 3.71−3.51 (m, 8H), 3.40−3.06 (m, 24H), 2.34 (s, 6H), 2.20 (s, 12H), 2.18 (s, 12H). ^{13}C NMR ($CDCl_3$): δ 155.5, 155.3, 154.4, 143.6, 143.4, 143.1, 137.5, 137.4, 136.1, 134.5, 134.4, 129.8, 129.5, 129.4, 127.4, 127.1, 127.0, 122.8, 121.0, 119.5, 54.0, 49.2, 49.1, 49.0, 48.2, 21.4, 21.3, 21.4. Anal. Calcd. for $C_{120}H_{128}N_{16}S_{10}O_{20}$: C, 59.19; H, 5.30; N, 9.20. Found: C, 59.6; H, 5.5; N, 9.0.

2,5,8,11,14-Pentaaza[15](6,6″)cyclo(2,2′:6′,2″)terpyridi-nophane Pentahydrobromide (L·5HBr). Compound **3** (1.65 g, 1.36 mmol) and phenol (17.9 g, 0.190 mol) were dissolved in 33% HBr−CH_3COOH (140 cm³). The reaction mixture was kept under stirring at 90 °C for 24 h until a precipitate was formed. The solid was filtered out and washed several times with CH_2Cl_2. The pentahydrobromide salt was recrystallized from an EtOH−water 3:1 mixture, yield 0.96 g (1.13 mmol, 83%). ^{1}H NMR (D_2O, pH = 2.23): δ 8.58−8.42 (m, 3H), 8.24 (d, $J = 7.69$ Hz, 2H), 8.14 (t, $J = 7.69$ Hz, 2H), 7.71 (d, $J = 7.69$ Hz, 2H), 4.69 (s, 4H), 3.65−3.46 (m, 8H), 3.40−3.29 (m, 4H), 3.29−3.17 (m, 4H). ^{13}C NMR (D_2O, pH 2.23): δ 152.5, 151.4, 151.1, 144.9, 140.6, 126.4, 125.3, 124.2, 51.8, 44.6, 44.1, 43.9, 43.6. MS m/z: 447.27 ([M + H]$^+$). Anal. Calcd. for $C_{25}H_{39}N_8Br_5$: C, 35.28; H, 4.62; N, 13.16. Found: C, 35.4; H, 4.6; N, 13.1.

2,5,8,11,14,32,35,38,41,44-Decaaza[30](6,6″)cyclo(2,2′:6′,2″)-bis-terpyridinophane Undecahydrobromide (5·11HBr). Compound **4** (0.56 g, 0.23 mmol) and phenol (6.06 g, 64.4 mmol) were dissolved in 33% HBr−CH_3COOH (45 cm³). The reaction mixture was kept under stirring at 90 °C for 24 h until a precipitate was formed. The solid was filtered out and washed several times with CH_2Cl_2. The undecahydrobromide salt was recrystallized from a 3:1 EtOH−water mixture, yield 0.24 g (0.14 mmol, 59%). ^{1}H NMR (D_2O, pH 3): δ 8.42 (d, $J = 7.97$ Hz, 4H), 8.25−8.10 (m, 6H), 7.95 (t, $J = 7.69$ Hz, 4H), 7.50 (d, $J = 7.69$ Hz, 4H), 4.59 (s, 8H), 3.80−3.64 (m, 16H), 3.61−3.49 (m, 16H). ^{13}C NMR (D_2O, pH 3): δ 153.4, 153.2, 150.8, 142.0, 140.0, 124.6, 123.9, 122.6, 51.8, 45.1, 44.5, 44.4, 44.0. MS m/z: 894.42 ([M + H]$^+$). Anal. Calcd. for $C_{50}H_{79}N_{16}Br_{11}$: C, 33.68; H, 4.46; N, 12.57. Found: C, 33.8; H, 4.6; N, 12.4.

[[ZnLH]$_2$(μ-OH)](ClO$_4$)$_5$. A solution of Zn(ClO$_4$)$_2$·6H$_2$O (4.5 mg, 0.012 mmol) in water (5 cm³) was slowly added to an aqueous solution (10 cm³) containing **L** (7.3 mg, 0.012 mmol). The pH was adjusted to 10 with 0.1 M NaOH, and then NaClO$_4$ (30 mg) and NaCl (20 mg) were added. Crystals of the complex suitable for X-ray analysis were obtained by slow evaporation at room temperature. Yield: 6 mg (64%). Anal. Calcd. for $C_{50}H_{71}Cl_5$-$Zn_2N_{16}O_{21}$: C, 38.99; H, 4.65; N, 14.55. Found: C, 38.9; H, 4.8; N, 14.7.

Caution! *Perchlorate salts of organic ligands and their metal complexes are potentially explosive; these compounds must be handled with great care.*

[[CdLH]$_2$(μ-Br)](ClO$_4$)$_5$·4H$_2$O. A solution of Cd(ClO$_4$)$_2$ (3.7 mg, 0.012 mmol) in water (5 cm³) was slowly added to an aqueous solution (10 cm³) containing **L** (7.3 mg, 0.012 mmol). The pH was adjusted to 8.3 with 0.1 M NaOH, and then NaClO$_4$ (30 mg) and

Table 1. Crystal Data and Structure Refinement for $\{[ZnLH]_2(\mu\text{-}OH)\}(ClO_4)_5$ (**6**) and $\{[CdLH]_2(\mu\text{-}Br)\}(ClO_4)_5\cdot4\ H_2O$ (**7**)

	6	7
empirical formula	$C_{50}H_{71}Cl_5N_{16}O_{21}Zn_2$	$C_{50}H_{78}BrCd_2Cl_5N_{16}O_{24}$
formula weight	1540.22	1769.24
temperature, K	298	298
wavelength, Å	1.54180	0.71069
space group	$P-1$	$P\ 21/c$
a, Å	12.647(2)	15.099(9)
b, Å	12.957(2)	19.567(5)
c, Å	20.815(7)	24.40(1)
α, deg	102.970(5)	
β, deg	92.79(2)	105.09(4)
γ, deg	105.61(1)	
volume, Å^3	3179.6(1)	6960(5)
Z	2	4
calculated density, mg/m^3	1.609	1.688
absorption coefficient, mm^{-1}	3.615	1.464
crystal size	$0.2 \times 0.2 \times 0.1$	$0.35 \times 0.3 \times 0.2$
final R indices [$I > 2\sigma(I)$]	R1^a = 0.0748, wR2 = 0.1535	R1^a = 0.0724, wR2 = 0.1905
R indices (all data)	R1^a = 0.1397, wR2 = 0.1840	R1^a = 0.1502, wR2 = 0.2225

^{a} R1 $= \Sigma||F_o| - |F_c||/\Sigma|F_o|$; wR2 $= [\ \Sigma w(F_o^2 - F_c^2)^2/\Sigma wF_o^4]^{1/2}$.

NaBr (25 mg) were added. Crystals of the complex suitable for X-ray analysis were obtained by slow evaporation at room temperature. Yield: 5.3 mg (57%). Anal. Calcd. for $C_{50}H_{78}Cl_5$-BrCd$_2$N$_{16}$O$_{24}$: C, 33.94; H, 4.44; N, 12.67. Found: C, 34.3; H, 4.3; N, 12.8.

X-ray Structure Analyses. Analyses on prismatic colorless single crystals of $\{[[ZnLH]_2(\mu\text{-}OH)\}(ClO_4)_5$ (**6**) and $\{[CdLH]_2(\mu\text{-}Br)\}(ClO_4)_5\cdot4\ H_2O$ (**7**) were carried out with Siemens P4 and Brucker MACH3 diffractometers, respectively. Details of data collections and structure refinements are summarized in Table 1. Both structures were solved by direct methods with the SIR97 program.[28] Refinements were performed by means of the full-matrix least-squares method with the SHELXL-97 program.[29]

X-ray Structure Determination of 6. Intensity data were empirically corrected for absorption (PSI-SCAN method). Anisotropic displacement parameters were used for all non-hydrogen atoms. Hydrogen atoms were introduced in calculated positions, and their thermal factors were refined, in agreement with the linked atoms. The hydrogen atom belonging to the hydroxide, localized in the Fourier difference map, was introduced in the calculation and was isotropically refined.

X-ray Structure Determination of 7. Data collection was carried out up to $2\theta = 40°$ because of the decay of the crystal (57% for the standard reflections). No absorption correction was performed. Anisotropic displacement parameters were used for all non-hydrogen atoms except for carbon atoms, which were isotropically refined. Hydrogen atoms were introduced in calculated positions, and their thermal factors were refined in agreement with the linked atoms. ISOR restrains (standard deviation 0.02) were applied to some oxygen atoms belonging to perchlorate anions or solvent molecules.

Potentiometric Measurements. All of the pH metric measurements (pH $= -\log$ [H$^+$]) were carried out in degassed 0.1 mol dm^{-3} NMe$_4$Cl solutions at 298.1 K using equipment and procedures that have already been described.[30] The combined Ingold 405 S7/120 electrode was calibrated as a hydrogen concentration probe by titrating known amounts of HCl with CO$_2$-free NMe$_4$OH

solutions and determining the equivalence point by Gran's method,[31] which allows one to determine the standard potential $E°$ and the ionic product of water (p$K_w = 13.83(1)$ at 298.1 K in 0.1 mol dm^{-3} NMe$_4$Cl). At least three potentiometric titrations were performed for each system in the pH range of 2.5−11. The ligand−metal molar ratio was varied from 0.5 to 1.8. To ascertain the formation of the dimeric species, the ligand and metal concentrations were simultaneously varied from 5×10^{-4} to 1×10^{-2}. The relevant emf data were treated by means of the computer program HYPER-QUAD.[32]
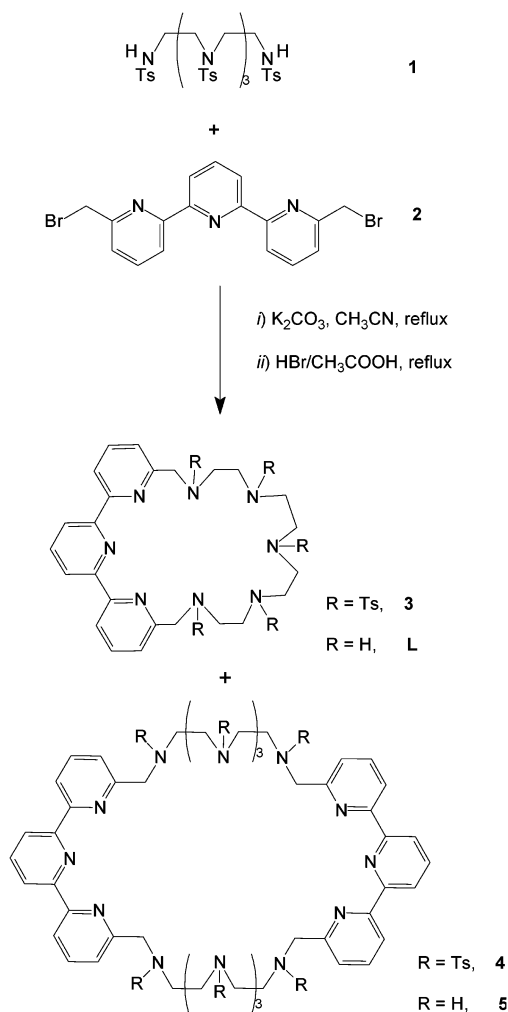
Results and Discussion

Ligand Synthesis. Ligand **L** was obtained according to a modification of the general procedure of Richman and Atkins[33] (Scheme 1). The reaction of 6,6″-bis(bromomethyl)-[2,2′:6′,2″]terpyridine[26] (**2**) with **1**,[25] carried out in anhydrous CH$_3$CN in the presence of K$_2$CO$_3$ as a base, afforded, after separation by column chromatography, tosylated macrocycles **3** and, in minor yield, **4**. (**3**, 57%; **4**, 17%).

Tosylated compounds **3** and **4** were finally deprotected in a 33% HBr/CH$_3$COOH mixture, according to a previously reported procedure,[21a] to afford ligands **L** and **5** as hydrobromide salts. The most interesting finding is the formation, in the critical cyclization step, of compound **4**, derived from a 2 + 2 cyclization. The same synthetic procedure, carried out with the corresponding bromomethyl derivatives of dipyridine or phenanthroline (6,6′-bis(bromomethyl)-2,2′-bipyridine and 2,9-bis(bromomethyl)-1,10-phenanthroline) formed only the 1 + 1 cyclization product, whereas the formation of the 2:2 macrocycles was not observed. Actually, rotation of the aromatic rings of terpyridine along the 2−2′ and 6′−2″ bonds may lead to conformations where the two bromomethyl reactive functions are placed at too large a distance to react simultaneously with the two terminal tosylated nitrogens of a single molecule of **1**, thus favoring the assembly of the 2:2 macrocycle. A similar 2 + 2

(28) Altomare, A.; Burla, M. C.; Camalli, M.; Cascarano, G. L.; Giacovazzo, C.; Guagliardi, A.; Moliterni, A. G. G.; Polidori, G.; Spagna, R. *J. Appl. Crystallogr.* **1999**, *32*, 115−119.

(29) Sheldrick, G. M. *SHELXL-97*; Göttingen, Germany, 1997.

(30) Bianchi, A.; Bologni, L.; Dapporto, P.; Micheloni, M.; Paoletti, P. *Inorg. Chem.* **1984**, *23*, 1201−1207.

(31) (a) Gran, G. *Analyst (London)* **1952**, *77*, 661−663. (b) Rossotti, F. J.; Rossotti, H. *J. Chem. Educ.* **1965**, *42*, 375−378.

(32) Gans, P.; Sabatini, A.; Vacca, A. *Talanta* **1996**, *43*, 1739−1753.

(33) Richman, J. E.; Atkins, T. J. *J. Am. Chem. Soc.* **1974**, *96*, 2268−2270.

Scheme 1

i) K_2CO_3, CH_3CN, reflux

ii) HBr/CH_3COOH, reflux

R = Ts, **3**

R = H, **L**

+

R = Ts, **4**

R = H, **5**

Figure 1. pH dependence of the H^1 NMR chemical shifts of **L** (a) and distribution diagrams of the protonated species of **L** (b).

cyclization between 6,6″-bis(bromomethyl)-[2,2′:6′,2″]terpyridine and tritosylated 1,4,7-triazaheptane was also observed by Picard et al.[17c] In this case, however, only the 2 + 2 cyclization product was obtained, probably because of the shorter length of the triamine precursor.

Ligand Protonation. The protonation equilibria of **L** were studied in a 0.1 mol dm^{-3} NMe$_4$Cl aqueous solution at 298.1 ± 0.1 K by means of potentiometric measurements in the pH range of 2−11. Ligand **L** can bind up to six protons in aqueous solutions and displays a marked grouping of the first three protonation constants (Log K_1 = 9.31(2), Log K_2 = 8.63(2), and Log K_3 = 7.27(2), K_x = [H$_x$**L**$^{x+}$]/[H$_{x-1}$**L**$^{(x-1)+}$]-[H$^+$]). A sharp decrease in basicity is observed between the third and the fourth protonation steps, the last three protonation constants being lower than 4 log units (Log K_4 = 3.92(2), Log K_5 = 2.80(2), and Log K_6 = 2.10(3)). This behavior, common in polyamine compounds,[34] is generally explained in terms of the minimization of the electrostatic repulsions between protonated amine groups. Terpyridine nitrogens, however, are characterized by far lower basicity than amine nitrogens;[24] therefore, it is expected that at least the first protonation steps take place on the aliphatic
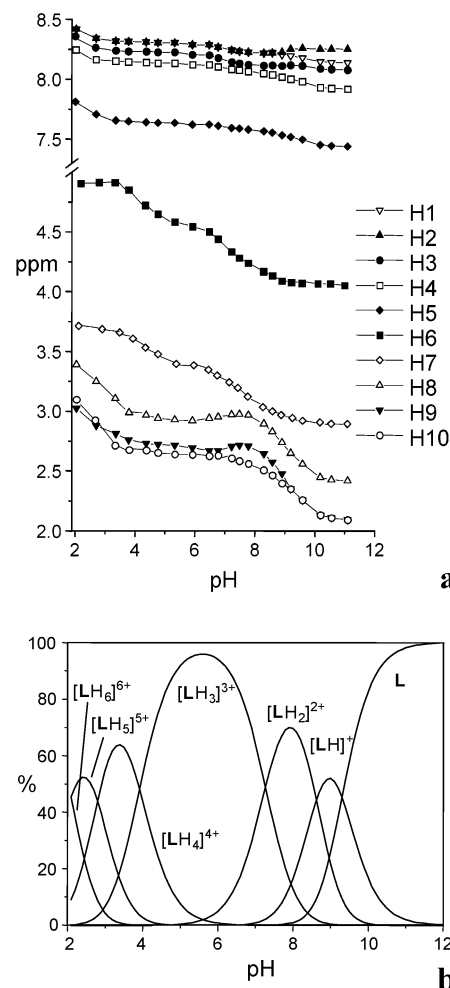
polyamine chain. To shed further light on the basicity properties of this ligand, we carried out ^{1}H NMR and UV−vis spectrophotometric measurements at different pH values in aqueous solutions. The ^{1}H spectrum of **L** at pH 11.6, where the free amine predominates in solution, displays five signals for the aliphatic protons and five for the aromatic ones, accounting for the C_{2v} time-averaged symmetry of the ligand, which is preserved over the entire pH range investigated (1.5−11.6). The pH dependence of the ^{1}H NMR signals is reported in Figure 1, together with the distribution diagram of the protonated species of **L**. In the pH range of 11.6−8, where the first two protons bind to the ligand, the resonances of H8, H9, and H10 in the α position, with respect to amine groups N2 and N3, display a marked downfield shift, whereas the other signals do not shift appreciably, indicating that the first two protonation steps occur on the central nitrogens of the pentaamine chain (Scheme 2). In other words, for the [H**L**]$^+$ and [H$_2$**L**]$^{2+}$ species, protonated forms with different proton localization among the N2 and N3 nitrogens coexist in solution, giving rise to a resulting downfield shift of H8, H9, and H10 signals. As already observed in phenanthroline-containing polyamine macrocycles,[21c−e] the higher proton affinity of N2 and N3 nitrogen atoms in comparison with that of N1 can be ascribed to the

(34) Bencini, A.; Bianchi, A.; García-España, E.; Micheloni, M.; Ramirez, J. A. *Coord. Chem. Rev.* **1999**, *118*, 97−156.

Scheme 2

Scheme 3
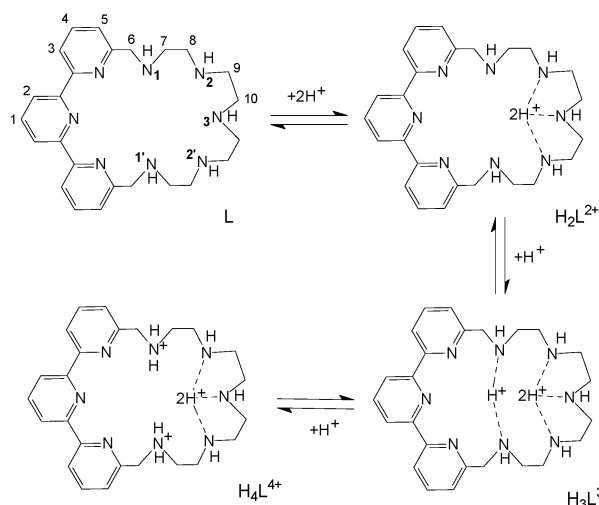
electron-withdrawing effect of the heteroaromatic unit on the adjacent N1 amine groups. The formation of the $[H_3L]^{3+}$ species, below pH 8, is accompanied instead by a downfield shift of H6 and H7, adjacent to the benzylic nitrogens N1, indicating that the third protonation step involves the benzylic amines. The fourth protonation step occurs on the N1 nitrogens, as shown by the downfield shift observed for the resonances of H6 and H7 below pH 5 (where the $[H_4L]^{4+}$ species is formed). The formation of the penta- and hexaprotonated species, below pH 3.5, is accompanied by a downfield shift of signals H8, H9, and H10 adjacent to the N2 and N3 amine groups. In the same pH region, however, the resonances of the terpyridine protons also display a downfield shift. These data suggest that the last two protonation steps involve the N2−CH₂−CH₂−N3 amine chain and the terpyridine unit.

This hypothesis is confirmed by the analysis of the UV absorption spectra recorded on solutions containing **L** at various pH values. It is well known that terpyridine undergoes two successive protonation processes in aqueous solution with pK_a values of 4.73 and 3.34.[35] In neutral aqueous solution, terpyridine presents a relatively broad absorption band centered at 290 nm ($\epsilon = 5500$ mol⁻¹ dm³ cm⁻¹, see Supporting Information). The protonation of terpyridine is accompanied by the appearance of a new band at ca. 325 nm ($\epsilon = 7950$ mol⁻¹ dm³ cm⁻¹), and a significant increase in the absorbance of the band at 290 nm ($\epsilon = 10\,200$ mol⁻¹ dm³ cm⁻¹).

The Hyperchem calculations[27] on terpyridine predict two $\pi\pi^*$ transitions at 323 and 286 nm, respectively, with a close-lying $n\pi^*$ transition at 315 nm. The transition moment associated with the lower-energy $\pi\pi^*$ transition is oriented along the short axis of terpyridine and is expected to be sensitive to protonation. However, the transition moment associated with the other $\pi\pi^*$ transition is oriented along the long axis of the molecule and should be less sensitive to protonation (Scheme 3). In unprotonated terpyridine, the proximity between the two allowed $\pi\pi^*$ transitions makes them appear as a single transition.
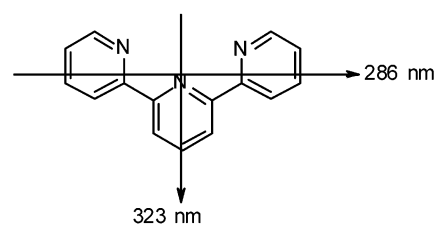
The calculation of the same transitions for monoprotonated terpyridine (at the central nitrogen) predicts the first $\pi\pi^*$ transition at 356 nm and the second $\pi\pi^*$ transition at 289 nm, that is, the $\pi\pi^*$ transition at the lowest energy is predicted to have a significant red shift upon protonation, whereas the $\pi\pi^*$ transition at the highest energy remains almost unchanged. As a consequence, the two transitions will appear very well separated. Despite the fact that the absolute values for the calculated transitions should be somewhat different in solution, the general picture for the observed allowed transitions is in accord with the experimental findings (Figure 2). However, the $n\pi^*$ transition arising from the n orbital of the protonated amine, which can now be considered to be a σ orbital, is expected to increase significantly in energy; consequently, changes in the observed extinction coefficient are also expected with protonation because the mixture between the states will be affected by changes in proximity of the forbidden and allowed states.

In the case of **L** (Figure 2A and B), this is observed only below pH 3.0, where $[H_5L]^{5+}$ and $[H_6L]^{6+}$ are formed in aqueous solutions. These results point out that the terpyridine unit is involved in protonation only in the highly charged $[H_5L]^{5+}$ and $[H_6L]^{6+}$ species.

The pH dependence of the fluorescence emission spectrum of **L** is reported in Figure 2C and D. At very low pH values, the fluorescence is characterized by two emission bands, centered at 360 and 335 nm, respectively. By increasing the pH, the band at 360 nm disappears, whereas the intensity of the band at 335 nm increases, becoming the dominant emission at pH 4.6. In acidic media, the pH dependence of the fluorescence emission is due to the relatively close energy of the $n\pi^*$ and $\pi\pi^*$ excited states of terpyridine.[36] By further increasing the pH, deprotonation of the $[H_3L]^{3+}$ species at neutral pH gives rise to a dramatic decrease in the fluorescence emission (Figure 2D). This result is in accord with the fact that in $[H_3L]^{3+}$ all aliphatic nitrogens are involved in proton binding and thus are not available for the emission quenching process. The removal of additional protons leads to the $[H_2L]^{2+}$ and $[HL]^+$ species, where the unprotonated benzylic nitrogens are now available for the quenching process.

The pH dependence of the fluorescence measured at the emission maximum of each $\pi\pi^*$ transitions, that is, at 330 and 360 nm, is also reported in Figure 2D. Because of the overlap of both bands, we subtract the contribution of the lower-energy emission band from the higher-energy band and vice versa (Figure 2D). According to this Figure, both

(35) Albano, G.; Balzani, V.; Constable E. C.; Maestri, M.; Smith, D. R. *Inorg. Chim. Acta* **1998**, *277*, 225−231.

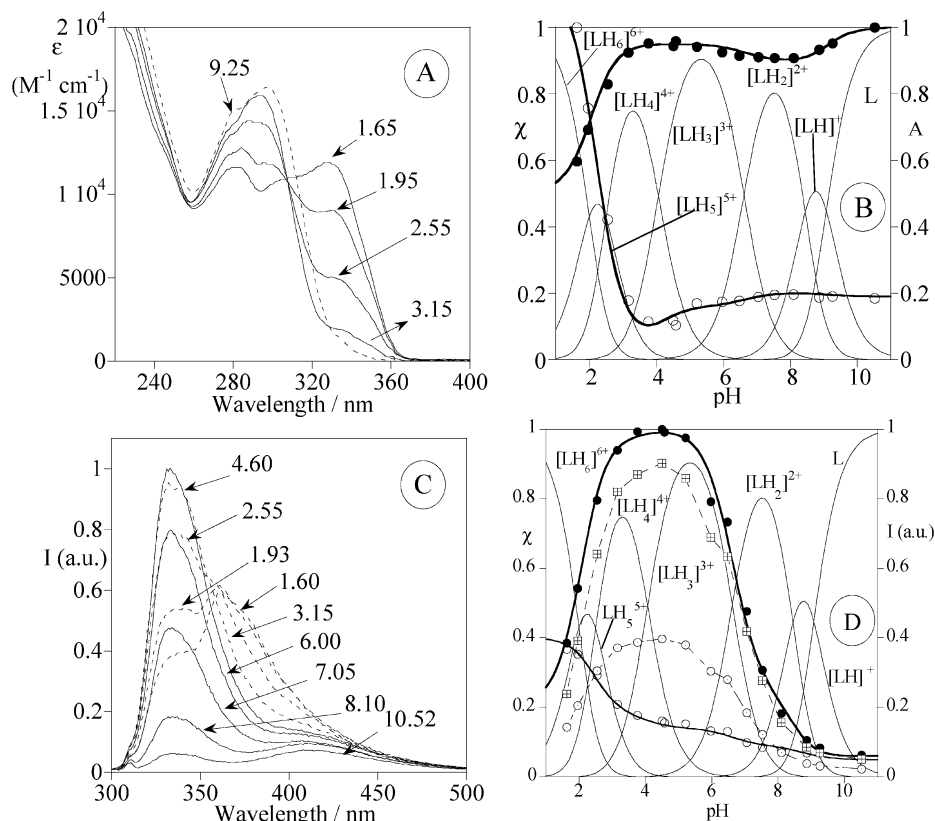(36) Sarkar, A.; Chakravorti, S. *J. Luminescence* **1995**, *63*, 143−148.

Figure 2. pH dependence of the absorption spectra of **L** (A) and absorbance at 295 (●) and 328 nm (○) (B), pH dependence of the fluorescence emission spectra (C), fluorescence intensity at 335 (—●—) and 390 nm (—○—) (D) and molar fractions (χ) of the protonated species of **L** (solid lines, left y axis) as a function of pH. (λ_{exc} 282 nm, [**L**] = 2.68 × 10^{-5} M, I = 0.1 M NMe$_4$Cl, 298 K). Part D also reports the fluorescence emission titration curves taken at the emission maximum of both $\pi\pi$ * transitions at 330 nm (cross inside square) and 360 nm (- - -○- - -). Because of the overlap of both curves, the values of the emission intensity at 330 and 360 nm were calculated by subtracting the contribution of the lower-energy emission band at 360 nm from the higher-energy band at 330 and vice versa.

$\pi\pi$* transitions show a similar profile. At lower pH values, the emission intensity is lower because the nπ* transition mixes with both $\pi\pi$* transitions, decreasing the fluorescence quantum yield.

These spectroscopic results point out that the protonated species of **L**, with the exception of [H$_5$**L**]$^{5+}$ and [H$_6$**L**]$^{6+}$, contain a nonprotonated terpyridine moiety, which can be used as a binding site for metals. However, an aliphatic pentaamine chain, if not protonated, generally displays a much better binding ability for metal cations than terpyridine. It is interesting, therefore, to analyze the coordination ability of ditopic ligand **L** toward metal cations and the structural features of the resulting complexes.

Synthesis and Crystal Structures of {[ZnLH]$_2$(μ-OH)}-(ClO$_4$)$_5$ (6) and {[CdLH]$_2$(μ-Br)}(ClO$_4$)$_5$·4H$_2$O (7). Complex **6** was obtained by the slow evaporation at room temperature of an aqueous solution containing Zn(ClO$_4$)$_2$·6H$_2$O and **L** in an equimolecular ratio and an excess of NaClO$_4$. The crystal structure of **6** consists of {[ZnLH]$_2$(μ-OH)}$^{5+}$ cations (Figure 3) and perchlorate anions. Bond lengths and angles for the metal coordination environment are listed in Table 2. The dimeric complex is formed by couples of [ZnLH]$^{3+}$ units linked by a bridging exogenous oxygen atom (O1) with an intermetallic distance of 3.709(3) Å. In principle, two different formulations can be proposed for this complex: {[ZnLH]$_2$(μ-OH)}$^{5+}$, where a OH$^-$ bridges the two metals and an uncoordinated nitrogen donor is
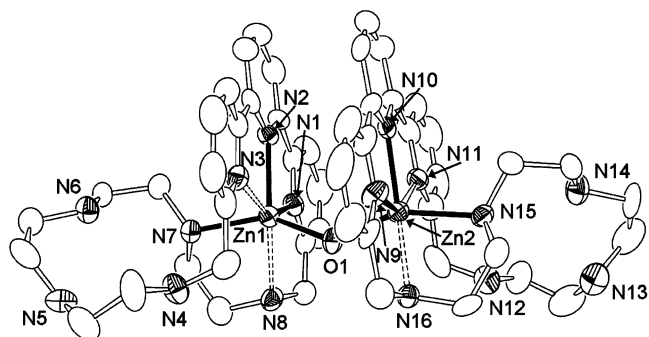

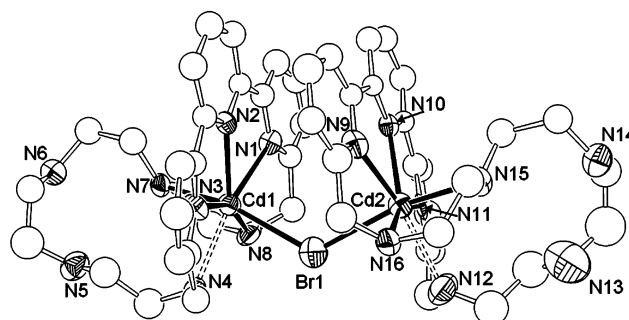**Figure 3.** ORTEP drawing of the {[ZnLH]$_2$(μ-OH)}$^{5+}$ cation.

protonated, or {[Zn**L**][Zn**L**H](μ-H$_2$O)]}$^{5+}$, with a water molecule bridging the two Zn(II) ions. Actually, the ΔF map did not allow us to localize the protons bound to the aliphatic nitrogen, and only a hydrogen bound to O1 is observed. However, the short Zn−O distances (Zn1−O1 1.959(10) Å, Zn2−O1 1.991 (10) Å) and the large Zn1−O1−Zn2 angle (139.7(6)°) lead us to propose the former formulation. In fact, several examples of a hydroxide anion bridging two Zn(II) metals have been reported, and the Zn−O distances range from 1.9 to 2.1 Å.[37] Water-bridged dimetal cores are less common, and larger Zn−O distances, ca. 2.3 Å, are found when a water molecule bridges the two metal centers.[38] However, the Zn−O−Zn angle in water-bridged dizinc complexes is lower than 110°,[38] whereas much larger Zn−O−Zn angles are found in hydroxo-bridged complexes.[37] In

Table 2. Selected Bond Lengths (Å) and Angles (deg) for {[Zn**L**H]$_2$(μ-OH)}(ClO$_4$)$_5$

Zn1−O1	1.959(10)	Zn2−O1	1.991(10)
Zn1−N1	2.135(9)	Zn2−N9	2.124(9)
Zn1−N2	2.136(8)	Zn2−N10	2.131(9)
Zn1−N3	2.368(9)	Zn2−N11	2.358(10)
Zn1−N7	2.119(8)	Zn2−N15	2.115(8)
Zn1−N8	2.424(8)	Zn2−N16	2.389(8)
O1−Zn1−N1	104.0(4)	O1−Zn2−N9	102.8(4)
O1−Zn1−N2	112.4(4)	O1−Zn2−N10	105.1(4)
O1−Zn1−N3	89.9(4)	O1−Zn2−N11	87.8(4)
O1−Zn1−N7	145.6(4)	O1−Zn2−N15	150.3(4)
O1−Zn1−N8	83.7(4)	O1−Zn2−N16	87.4(4)
N1−Zn1−N2	75.5(4)	N9−Zn2−N10	75.9(4)
N1−Zn1−N3	147.3(4)	N9−Zn2−N11	147.4(4)
N1−Zn1−N7	98.0(3)	N9−Zn2−N15	98.3(3)
N1−Zn1−N8	73.8(4)	N9−Zn2−N16	74.7(4)
N2−Zn1−N3	71.8(4)	N10−Zn2−N11	71.6(4)
N2−Zn1−N7	98.4(3)	N10−Zn2−N15	100.2(3)
N2−Zn1−N8	148.1(4)	N10−Zn2−N16	150.0(4)
N3−Zn1−N7	85.5(3)	N11−Zn2−N15	85.5(3)
N3−Zn1−N8	138.0(3)	N11−Zn2−N16	137.2(3)
N7−Zn1−N8	77.4(3)	N15−Zn2−N16	78.2(3)
Zn1−O1−Zn2	139.7(6)		

both [Zn**L**H]$^{3+}$ units, the overall conformation of **L** and the coordination geometry of the metals are very similar. Each Zn(II) ion is coordinated to the three aromatic nitrogens, two secondary nitrogens belonging to the same macrocyclic unit (N7 and N8 for Zn1 and N15 and N16 for Zn2), and the bridging hydroxide anion. However, two nitrogen donors (N3 and N8 for Zn1, N11 and N16 for Zn2) weakly interact with the metal, being coordinated at a rather large distance (>2.35 Å). The resulting metal-coordination environment can be best described as a distorted octahedron. The two ligand molecules in the {[Zn**L**H]$_2$(μ-OH)}$^{5+}$ complex cations also interact via face-to-face π stacking between the two terpyridine units. These moieties are almost parallel, with a dihedral angle of 3.8(2)° between the mean planes defined by each terpyridine unit and an interplanar distance of 3.5 Å. The two stacked aromatic units are slightly rotated (13°) around the Zn−Zn axis.

Considering the ligand conformation, the cyclic framework is folded along the axis linking the benzylic carbon atoms, forming dihedral angles of 49.1(2)° ([Zn1**L**H]$^{3+}$ unit) and 54.0(3)° ([Zn2**L**H]$^{3+}$) between the mean planes defined by

(37) A large number of structurally characterized μ-OH dizinc complexes have been reported in the literature. Some exemplifying papers are (a) Bell, M.; Edwards, A. J.; Hoskins, B. F.; Kachab, E. H.; Robson, R. *J. Am. Chem. Soc.* **1989**, *111*, 3603−3610. (b) Grannas, M. J.; Hoskins, B. F.; Robson, R. *Chem. Commun.* **1990**, 1644−1646. (c) Grannas, M. J.; Hoskins, B. F.; Robson, R. *Inorg. Chem.* **1994**, *33*, 1071−1079. (d) Tan, L. H.; Taylor, M. R.; Wainwright, K. P.; Duckworth, P. A. *J. Chem. Soc., Dalton Trans.* **1993**, 2921−2928. (e) Hermann, J.; Erxleben, A. *Inorg. Chim. Acta* **2000**, *304*, 125−129. (f) Bazzicalupi, C.; Bencini, A.; Bianchi, A.; Fusi, V.; Paoletti, P.; Valtancoli, B. *Chem. Commun.* **1994**, 881−882. (g) Bazzicalupi, C.; Bencini, A.; Bianchi, A.; Fusi, V.; Mazzanti, L.; Paoletti, P.; Valtancoli, B. *Inorg. Chem.* **1995**, *34*, 3003−3013. (h) Bazzicalupi, C.; Bencini, A.; Bianchi, A.; Fusi, V.; Paoletti, P.; Piccardi, G.; Valtancoli, B. *Inorg. Chem.* **1995**, *34*, 5622−5630. (i) Asato, E.; Furutachi, H.; Kawahashi, T.; Mikuriya, M. *J. Chem. Soc., Dalton Trans.* **1995**, 3897−3904.
(38) Only a few examples of μ-H$_2$O dizinc complexes have been reported: (a) Wolodkiewicz, W.; Glowiak, T. *Pol. J. Chem.* **2001**, *75*, 299−306. (b) Johnson, J. A.; Olmstead, M. M.; Stolzenberg, A. M.; Balch, A. L. *Inorg. Chem.* **2001**, *40*, 5585−5595. (c) Barrios, A. M.; Lippard, S. J. *Inorg. Chem.* **2001**, *40*, 1060−1064.

Figure 4. ORTEP drawing of the {[Cd**L**H]$_2$(μ-Br)}$^{5+}$ cation.

Table 3. Selected Bond Lengths (Å) and Angles (deg) for {[Cd**L**H]$_2$(μ-Br)}(ClO$_4$)$_5$·4H$_2$O

Cd1−Br1	2.753(3)	Cd2−Br1	2.720(3)
Cd1−N1	2.416(14)	Cd2−N9	2.386(14)
Cd1−N2	2.409(14)	Cd2−N10	2.422(13)
Cd1−N3	2.365(15)	Cd2−N11	2.404(15)
Cd1−N4	2.528(15)	Cd2−N12	2.577(17)
Cd1−N7	2.480(14)	Cd2−N15	2.430(15)
Cd1−N8	2.445(16)	Cd2−N16	2.444(15)
Br1−Cd1−N1	97.6(3)	Br1−Cd2−N9	92.0(4)
Br1−Cd1−N2	107.4(3)	Br1−Cd2−N10	100.9(3)
Br1−Cd1−N3	87.6(4)	Br1−Cd2−N11	87.2(3)
Br1−Cd1−N4	78.5(3)	Br1−Cd2−N12	84.9(4)
Br1−Cd1−N7	160.3(3)	Br1−Cd2−N15	160.9(3)
Br1−Cd1−N8	89.1(4)	Br1−Cd2−N16	87.1(4)
N1−Cd1−N2	65.2(4)	N9−Cd2−N10	66.8(5)
N1−Cd1−N3	131.8(5)	N9−Cd2−N11	133.1(5)
N1−Cd1−N4	159.5(5)	N9−Cd2−N12	157.3(6)
N1−Cd1−N7	84.4(5)	N9−Cd2−N15	86.7(5)
N1−Cd1−N8	70.7(5)	N9−Cd2−N16	70.0(5)
N2−Cd1−N3	67.5(5)	N10−Cd2−N11	67.4(5)
N2−Cd1−N4	135.2(5)	N10−Cd2−N12	135.9(6)
N2−Cd1−N7	91.3(5)	N10−Cd2−N15	96.1(5)
N2−Cd1−N8	134.4(5)	N10−Cd2−N16	136.2(5)
N3−Cd1−N4	68.5(5)	N11−Cd2−N12	69.4(6)
N3−Cd1−N7	105.8(5)	N11−Cd2−N15	107.6(5)
N3−Cd1−N8	157.5(5)	N11−Cd2−N16	156.4(5)
N4−Cd1−N8	89.1(5)	N12−Cd2−N15	89.0(6)
N4−Cd1−N7	92.8(5)	N12−Cd2−N16	87.3(6)
N7−Cd1−N8	73.0(5)	N15−Cd2−N16	74.5(5)
Cd1−Br1−Cd2	124.95(10)		

the terpyridine units and by the five aliphatic nitrogens, respectively.

Our attempts to obtain crystals, suitable for X-ray analysis, of the Cu(II), Cd(II), and Pb(II) complexes with **L**, following the simple procedure used for the Zn(II) complex, failed. In the case of Cd(II), however, the addition of NaBr to an aqueous solution of **L** and Cd(II) in an equimolecular ratio leads to the crystallization of {[Cd**L**H]$_2$(μ-Br)}(ClO$_4$)$_5$·4H$_2$O (**7**), which was structurally characterized. The crystal structure of **7** consists of {[Cd**L**H]$_2$(μ-Br)}$^{5+}$ complex cations, perchlorate anions, and water solvent molecules. The {[Cd**L**H]$_2$(μ-Br)}$^{5+}$ cation is composed of a [Cd**L**H]$^{3+}$ monomeric unit, coupled by a bridging bromide anion (Figure 4). The two metals are located 4.854(3) Å apart. As in **6**, the two metal ions display a similar coordination environment; each metal is coordinated to the three heteroaromatic nitrogens and three secondary nitrogens belonging to the same macrocyclic moiety (N4, N7, and N8 for Cd1 and N12, N15, and N16 for Cd2) (Figure 4 and Table 3). An amine group (N4 for Cd1, N12 for Cd2) is bound at a longer distance with respect to the remaining coordinated

Table 4. Stability Constants (log K) of the Metal Complexes with **L** (NMe$_4$Cl 0.1 M, 298.1 K)

reaction	Cu(II)	Zn(II)	Cd(II)	Pb(II)
M^{2+} + **L** = [M**L**]$^{2+}$			10.1(1)	8.6(1)
[M**L**]$^{2+}$ + H$^+$ = [MH**L**]$^{3+}$			9.6(1)	9.64(7)
M^{2+} + **L** + H$^+$ = MH**L**]$^{3+}$		20.76(3)		
[M**L**H]$^{3+}$ + H$^+$ = [M**L**H$_2$]$^{4+}$			6.1(1)	5.81(6)
[M**L**H$_2$]$^{4+}$ + H$^+$ = [M**L**H$_3$]$^{5+}$				4.70(8)
[M**L**H]$^{3+}$ + 2H$^+$ = [M**L**H$_3$]$^{5+}$		7.85(7)		
[M**L**]$^{2+}$ + OH$^-$ = [M**L**(OH)]$^+$				3.7(1)
2M^{2+} + 2**L** + H$^+$ = [M$_2$**L**$_2$H]$^{5+}$		35.5(1)		
2M^{2+} + 2**L** + H$_2$O = [M$_2$**L**$_2$(OH)]$^{3+}$ + H$^+$		15.8(1)		
2M^{2+} + 2**L** = [M$_2$**L**$_2$]$^{4+}$	39.1(1)			
[M$_2$**L**$_2$]$^{4+}$ + H$^+$ = [M$_2$**L**$_2$H]$^{5+}$	7.2(1)			
[M$_2$**L**$_2$H]$^{5+}$ + H$^+$ = [M$_2$**L**$_2$H$_2$]$^{6+}$	6.3(1)			
[M$_2$**L**$_2$]$^{4+}$ + OH$^-$ = [M$_2$**L**$_2$(OH)]$^{3+}$	3.33(1)			
2M^{2+} + **L** = [M$_2$**L**]$^{4+}$	26.00(6)		16.6(2)	14.2(1)
2M^{2+} + **L** + OH$^-$ = [M$_2$**L**(OH)]$^{3+}$		22.9(1)		
[M$_2$**L**]$^{4+}$ + OH$^-$ = [M$_2$**L**(OH)]$^{3+}$	4.8(1)			5.4(1)
[M$_2$**L**(OH)]$^{3+}$ + OH$^-$ = [M$_2$**L**(OH)$_2$]$^{2+}$	3.5(1)			

nitrogens. The Cd(II) coordination-geometry environments can be described as a distorted pentagonal bipyramid where the terpyridine nitrogens and the benzylic amine groups (N4 and N8 for Cd1 and N12 and N16 for Cd2) define the equatorial plane and the bridging bromide anion and N7 (Cd1) and N15 (Cd2) occupy the apical positions. One of the uncoordinated N5 and N6 amine groups of [Cd1**L**H]$^{3+}$ (N13 and N14 in [Cd2**L**H]$^{3+}$) is protonated. Considering the ligand conformation, each macrocyclic unit assumes a similar conformation to that observed in the [Zn**L**H]$^{3+}$ units of **6**, folded along the axis joining the benzylic carbons with dihedral angles of 64.4(4) and 64.6(4)° between the mean planes defined by the aromatic moiety and by the aliphatic amine groups of [Cd1**L**H]$^{3+}$ and [Cd2**L**H]$^{3+}$, respectively.

Whereas in **6** the pyridine units of each [Zn**L**H]$^{3+}$ moiety are essentially coplanar, in **7** the pyridine rings display a larger deviation from coplanarity, with a dihedral angle of 17.2(6)° between the planes of pyridine units N3 and N2 in [Cd1**L**H]$^{3+}$ (14.5(5)° between the planes of the N10 and N11 pyridine units in [Cd2**L**H]$^{3+}$).

Similar to **6**, the two terpyridine units interact via π stacking, with a distance between the mean planes defined by each heteroaromatic unit of 3.5 Å; in **7**, however, these planes form a larger dihedral angle than in **6** (10.0(4) vs 3.8(2)°). Furthermore, in **7**, the two terpyridine units are rotated 45° on the intermetallic axis (13° in **6**). These structural features account for a weaker π-stacking interaction in Cd(II) complex **7** than in Zn(II) complex **6**.

The most interesting feature of the **6** and **7** complexes is their dimeric structure, formed by two different [M**L**H]$^{3+}$ (M = Zn or Cd) protonated complexes, coupled by a bridging anion and π-stacking interactions between the two terpyridine units. The formation of Zn(II) or Cd(II) dimeric complexes, derived from two single mononuclear complexes coupled by bridging hydroxide[39] or halide anions,[40] is common, at least in the solid state. Examples of the association of two monomeric complexes through bridging anions and simultaneous π-stacking interactions are rarer.[41] With few exceptions,[42] the [M$_2$(μ-OH)]$^{3+}$ (M = Zn or Cd) clusters are cleaved in solution, where metal solvation leads to the disruption of the dimeric species to give simple 1:1 com-

plexes. An additional peculiar characteristic of the present Zn(II) and Cd(II) complexes is the fact that the monomeric units forming the {[Zn**L**H]$_2$(μ-OH)}$^{5+}$ and {[Cd**L**H]$_2$(μ-Br)}$^{5+}$ assemblies are protonated. This would give an unfavorable contribution to the assembly of the [M$_2$(μ-OH)]$^{3+}$ clusters because of the increased electrostatic repulsions between the two monomeric complexes. The formation of dimeric complexes, therefore, suggests a synergetic action of the bridging anion and the π-stacking interactions between two large terpyridine units. These considerations would suggest that the dimeric stucture of the complexes could be

(39) (a) Rosi, N. L.; Eddaoudi, M.; Kim, J.; O'Keeffe, M.; Yaghi, O. M. *Angew. Chem., Int. Ed.* **2002**, *41*, 284−287. (b) Tao, J.-X.; Shi, J.-X.; Tong, M.-L.; Zhang, X.-X.; Chen, X.-H. *Inorg. Chem.* **2001**, *40*, 6328−6330. (c) Mikuriya, M.; Minowa, K. *Inorg. Chem. Commun.* **2000**, *3*, 227−230. (d) Berreau, L. M.; Allred, R. A.; Makowska-Grzyska, M. M.; Arif, A. M. *Chem. Commun.* **2000**, 1423−1424. (e) Hammes, B. S.; Carrano, C. J. *Chem. Commun.* **2000**, 1635−1636. (f) Gerrard, L. A.; Wood, P. T. *Chem. Commun.* **2000**, 2107−2108. (g) Looney, A.; Han, R.; Gorrell, I. B.; Cornebise, M.; Yoon, K.; Parkin, G.; Rheingold, A. L. *Organometallics* **1995**, *14*, 274−288. (h) Flassbeck, C.; Wieghardt, K.; Bill, E.; Butzlaff, C.; Trautwein, A. X.; Nuber, B.; Weiss, J. *Inorg. Chem.* **1992**, *31*, 21−26. (i) Murthy, N. N.; Karlin, K. D. *Chem. Commun.* **1993**, 1236−1238. (j) Branscombe, N. D. J.; Blake, A. J.; Marin-Becerra, A.; Li, W.; Parsons, S.; Ruiz-Ramirez, L.; Schroder, M. *Chem. Commun.* **1996**, 2573−2574. (k) Chaudhuri, P.; Stockheim, C.; Wieghardt, K.; Deck, W.; Gregorzik, R.; Vahrenkamp, H.; Nuber, B.; Weiss, J. *Inorg. Chem.* **1992**, *31*, 1451−1457.

(40) (a) Vaidhyanathan, R.; Natarajan, S.; Rao, C. N. R. *Chem. Mater.* **2001**, *13*, 3524−3533. (b) Lartigue-Bourdeau, C.; Chanh, N. B.; Duplessix, R.; Gallois, B. *J. Phys. Chem. Solids* **1993**, *54*, 349−356. (c) Gonzalez-Duarte, P.; Clegg, W.; Casals, I.; Sola, J.; Rius, J. *J. Am. Chem. Soc.* **1998**, *120*, 1260−1266. (d) Puget, R.; Jannin, M.; De Brauer, C.; Perret, R. *Acta Crystallogr., Sect. C* **1991**, *47*, 1803−1805.

(41) (a) Blake, A. J.; Devillanova, F. A.; Garau, A.; Harrison, A.; Isaia, F.; Lippolis, V.; Tiwary, S. K.; Schroeder, M.; Verani, G.; Whittaker, G. *J. Chem. Soc., Dalton Trans.* **2002**, 4389−4394. (b) Cheng, M.; Moore, D. R.; Reczek, J. J.; Chamberlain, B. M.; Lobkovsky, E. B.; Coates, G. W. *J. Am. Chem. Soc.* **2001**, *123*, 8738−8749. (c) Plater, M. J.; Foreman, M. R. St. J.; Gelbrich, T.; Hursthouse, M. B. *J. Chem. Soc., Dalton Trans.* **2000**, 1995−2000. (d) Tao, J.; Tong, M.-L.; Shi, J.-X.; Chen, X.-M.; Weng Ng, S. *Chem. Commun.* **2000**, 2043−2044. (e) Fusch, E. C.; Lippert, B. *J. Am. Chem. Soc.* **1994**, *116*, 7204−7209. (f) Mamula, O.; von Zelewsky, A.; Bark, T.; Stoeckli-Evans, H.; Neels, A.; Bernardinelli, G. *Chem.−Eur. J.* **2000**, *6*, 3575−3585.

(42) (a) Adams, H.; Bastida, R.; Fenton, D. E.; Macias, A.; Spey, S. E.; Valencia, L. *J. Chem. Soc., Dalton Trans.* **1999**, 4131−4137. (b) Chu, F.; Smith, J.; Lynch, V. M.; Anslyn, E. V. *Inorg. Chem.* **1995**, *34*, 5689−5690. (c) Furuta, H.; Ishizuka, T.; Osuka, A. *J. Am. Chem. Soc.* **2002**, *124*, 5622−5623.

also maintained in solution; we decided, therefore, to carry out a potentiometric and spectrophotometric study on metal complexation with **L** in aqueous solution.

Cu(II), Zn(II), Cd(II), and Pb(II) Coordination in Aqueous Solution. The formation of the Cu(II), Zn(II), Cd-(II), and Pb(II) complexes with **L** was investigated by means of potentiometric and UV–vis and fluorescence emission spectrophotometric measurements in aqueous solution (NMe$_4$-Cl 0.1 M, 298.1 K). The species formed and the corresponding stability constants of the complexes, potentiometrically determined, are reported in Table 4. As shown in Figure 5, with a metal-to-ligand 1:1 molar ratio, complex formation occurs at acidic pH values, indicating the formation of stable metal chelates with **L**. The most interesting finding in Table 4 and Figure 5, however, is the different coordination behavior of **L** toward Cu(II) and Zn(II) with respect to Cd(II) and Pb(II). In the case of Zn(II), metal complexation occurs at acidic pH values to give mononuclear protonated complexes ([ZnLH$_3$]$^{5+}$ and [ZnLH]$^{3+}$). The formation of the [ZnLH$_2$]$^{4+}$ species is not observed by potentiometry. This behavior is often found in metal complexes with polyamine ligands and is related to the fact that the two deprotonation steps that afford the [ZnLH]$^{3+}$ species from [ZnLH$_3$]$^{5+}$ take place almost simultaneously; therefore, only the overall equilibrium [ZnLH$_3$]$^{5+}$ = [ZnLH]$^{3+}$ + 2H$^+$ can be detected. Deprotonation of the [ZnLH]$^{3+}$ species takes place at slightly alkaline pH values and affords the dimeric species [Zn$_2$L$_2$H]$^{5+}$. The crystal structure of the {[ZnLH]$_2$(μ-OH)}$^{5+}$ complex would suggest that in this dimeric species observed in solution two monomeric Zn(II) complexes are associated via a bridging hydroxide and π-stacking interactions between two terpyridine units, whereas the polyamine chain of each [ZnL] unit is monoprotonated. In other words, the potentiometrically determined [Zn$_2$L$_2$H]$^{5+}$ stoichiometry originates in the association of two [ZnLH]$^{3+}$ units coupled by a bridging OH$^-$ anion and π-stacking interactions. Finally, further complex deprotonation affords, above pH 10, the [Zn$_2$L$_2$(OH)]$^{3+}$ dimer. The presence in solution of π-stacking interactions, which contribute to the stabilization of the dimeric species, is confirmed by the analysis of the UV spectra recorded in solutions containing **L** and Zn(II) in a 1:1 molar ratio at different pH values (Figure 6). As in the case of proton binding, metal coordination by the heteroaromatic unit gives marked changes in the absorption spectra of ligand **L**, with the appearance of new structured red-shifted absorption at ca. 330 nm. This new band can be used as a diagnostic tool to prove the effective involvement of terpyridine nitrogens in metal binding. According to Figure 6a, the formation of a new red-shifted band at 335 nm is observed upon Zn(II) complexation above pH 4, where the [ZnLH$_3$]$^{5+}$ and [ZnLH]$^{3+}$ complexes are formed. These spectral features do not change up to pH 6; by further increasing the pH, the band at 335 nm displays a marked decrease in absorbance, accompanied by the formation of a new blue-shifted band at 310 nm (Figure 6b). This effect is generally observed in the presence of π-stacking interactions
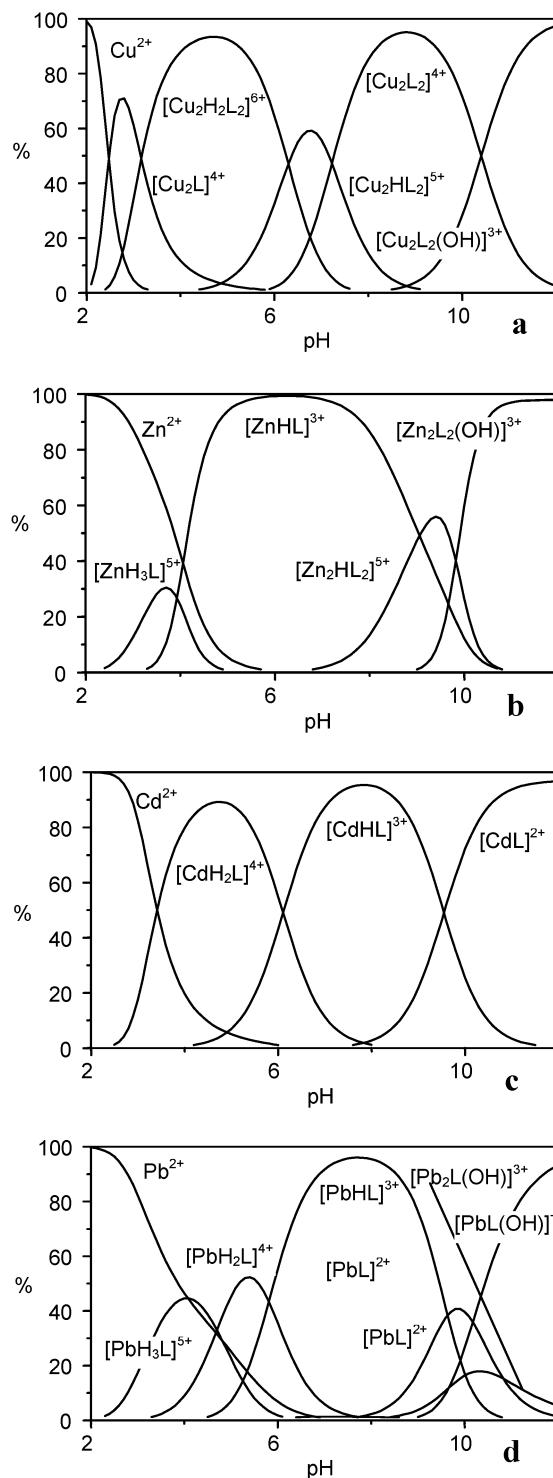
Figure 5. Distribution diagrams of the species for the systems **L**\Cu(II) (a), **L**\Zn(II) (b), **L**\Cd(II) (c), and **L**\Pb(II) (d) (NMe$_4$Cl 0.1 mol dm^{-3}, 298.1 K, [**L**] = [M^{2+}] = 1 × 10^{-3} M).

between aromatic moieties.[43] In our case, Figure 6c clearly shows that the decrease in absorbance of the band at 335 nm occurs with the formation of the [Zn$_2$L$_2$H]$^{5+}$ and [Zn$_2$L$_2$-(OH)]$^{3+}$ dimeric complexes, indicating the essential role of

(43) (a) Ern, J.; Bock, A.; Oddos-Marcel, L.; Rengel, H.; Wegner, G.; Trommsdorff, H. P.; Kryschi, C. *J. Phys. Chem. A* **1999**, *103*, 2446–2450 and references therein. (b) Angiolini, A.; Caretti, D.; Giorgini, L.; Salatelli, E. *e-Polym.* **2001**, *21*, 1–12 and references therein.
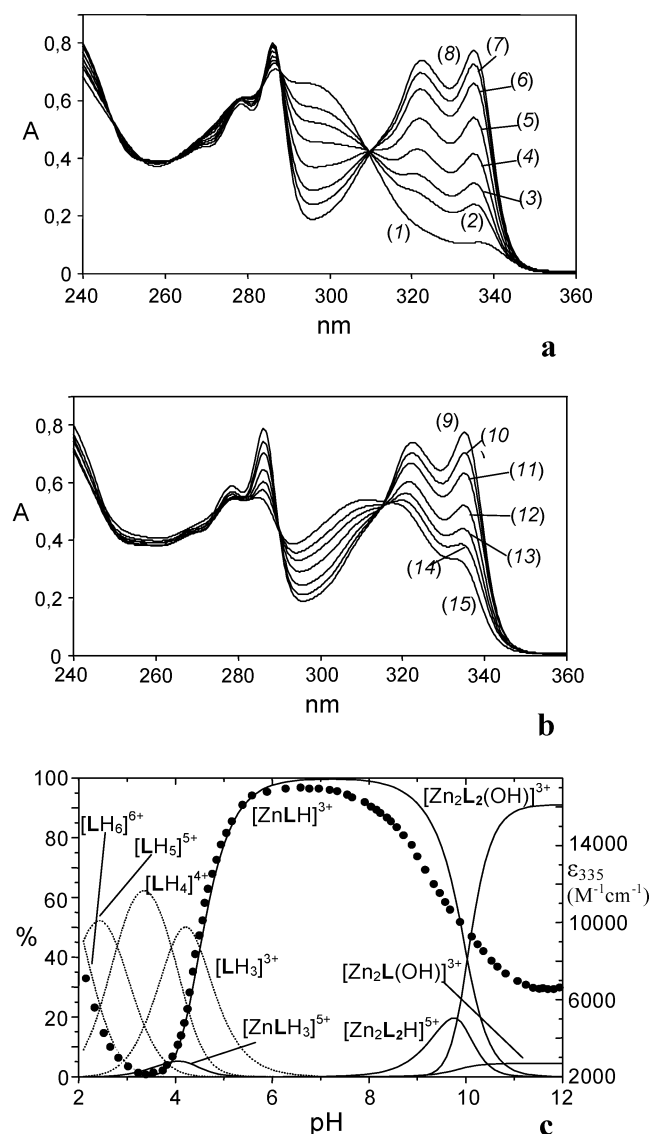
Figure 6. UV−vis spectra recorded on aqueous solutions containing **L** and Zn(II) in a 1:1 molar ratio (a) in the pH range 3−6.5 [(*1*) pH 3.54, (*2*) 3.99, (*3*) 4.12, (*4*) 4.27, (*5*) 4.45, (*6*) 4.70, (*7*) 4.93, (*8*) 6.40] (0.1 mol dm^{-3} NMe$_4$Cl, T = 298.1 K) and (b) in the pH range 6−12: [(*9*) pH 6.40, (*10*) 8.57, (*11*) 9.00, (*12*) 9.57, (*13*) 10.12, (*14*) 10.53, (*15*) 11.52] (0.1 mol dm^{-3} NMe$_4$Cl, T = 298.1 K). (c) pH dependence of the absorbance at 335 nm of **L** in the presence of Zn(II) in a 1:1 molar ratio (●, right y axis) ([**L**] = 5.1 × 10^{-5} M, 0.1 M NMe$_4$Cl, 298.1 K), superimposed on the distribution diagram of the protonated (··) and complexed (—) species of the ligand.

π-stacking interactions in the assembly of these dimeric species. It is well known that the formation of dimeric complexes from monomeric ones is generally favored by increased complex concentrations. Actually, plots of the speciation diagrams with increasing ligand and metal concentrations (1:1 molar ratio) clearly show the formation of increased percentages of the dimeric complexes (Figure S2, Supporting Information). However, above pH 9, the ϵ value measured at 335 nm at a given pH decreases with increasing overall complex concentration, whereas the ϵ value at 310 nm increases, pointing out that the percentage of dimeric species increases with complex concentration, in accord with the speciation curves derived from the potentiometric results. Plots of the 335 and 310 nm ϵ values as a function of the overall percentages of the dimeric complexes at pH 9.9 and

11, calculated on the basis of the potentiometric data (Figure S3), show a linear decrease in the absorbance at 335 nm and a linear increase in the absorbance at 310 nm with increasing concentration of the dimeric complexes, confirming that the observed variation of the spectral features is indeed due to the assembly of π-stacked dimers.

These spectrophotometric results are not conclusive with regard to the presence of a bridging hydroxide anion between the two metals; however, it should be noted that π-stacking interactions are generally too weak to assemble two charged [ML]$^{2+}$ moieties in solution. This consideration gives confidence to the proposed structure for the dimeric Zn(II) species formed in solution.

The dimeric complexes are a peculiar feature of Zn(II) coordination by **L** in the alkaline pH region; the dimeric structure, however, is disrupted below pH 8, where the increased protonation of the ligand enhances the electrostatic repulsions between the two [ZnL] units.

In the case of Cu(II) complexation, a marked red shift of the terpyridine absorption, up to 330 nm, accompanies the formation, at acidic pH values, of the dinuclear [Cu$_2$L]$^{4+}$ complex (Figure 5a), where one Cu(II) ion is likely coordinated to the heteroaromatic nitrogens. As in the case of Zn(II), the assembly of the dimeric complex [Cu$_2$L$_2$H$_2$]$^{6+}$ at pH 4 gives rise to a new blue-shifted band, with a maximum at 310 nm, indicating, once again, the presence of π-stacking interactions between the terpyridine moieties. By increasing the pH, the absorption spectra do not change upon deprotonation of [Cu$_2$L$_2$H$_2$]$^{6+}$ to give the [Cu$_2$L$_2$H]$^{5+}$ and [Cu$_2$L$_2$(OH)]$^{3+}$ complexes. Most likely, these dimeric species contain two [CuL] units held together by a bridging hydroxide anion and π-stacking interactions, as already observed in the case of the corresponding Zn(II) complexes. The dimeric [Cu$_2$L$_2$(OH)]$^{3+}$ and [Cu$_2$L$_2$]$^{4+}$ complexes display a single d−d absorption band at 602 nm (ϵ = 202 mol^{-1} dm^3 cm^{-1}). These spectral features are not influenced by the formation of the [Cu$_2$L$_2$H$_2$]$^{6+}$ and [Cu$_2$L$_2$H]$^{5+}$ protonated species. On the contrary, the formation of the dinuclear [Cu$_2$L]$^{4+}$ complex gives rise to a red shift of the d−d band (λ$_{max}$ = 647, ϵ = 336 mol^{-1} dm^3 cm^{-1}), as expected considering that the eight nitrogen donors of the macrocycle cannot fulfill the coordination sphere of both metals, leading to lower coordination numbers for the Cu(II) ions in this complex.

Different from Zn(II), this dimeric assembly is a common feature of all of the complexes with a 1:1 metal-to-ligand molar ratio. The absence of discrete 1:1 Cu(II) complexes can be tentatively related to a higher affinity of the coordinated Cu(II) ion for the hydroxide anion and/or to the presence of stronger π-stacking interactions, with a consequently higher stability of the [Cu$_2$(μ-OH)L$_2$] clusters. Only the formation of dinuclear [Cu$_2$L]$^{4+}$ complexes leads to the disruption of the dimeric structure because of the higher electrostatic repulsion between two tetracharged dinuclear species.

The Cd(II) and Pb(II) complexes display a different behavior. The potentiometric measurements, in fact, do not show the formation of dimeric assemblies, and simple
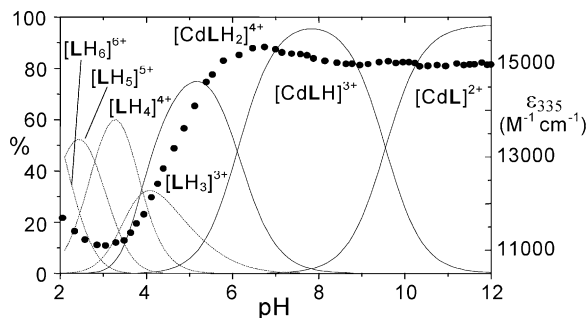
Figure 7. pH dependence of the absorbance at 335 nm of **L** in the presence of Cd(II) in a 1:1 molar ratio (●, right *y* axis) ([**L**] = 5.15 × 10⁻⁵ M, 0.1 M NMe₄Cl, 298.1 K) superimposed on the distribution diagram of the protonated (···) and complexed (—)species of the ligand.

mononuclear complexes are the main species present in solution containing the metal and the ligand in a 1:1 molar ratio. Cd(II) and Pb(II) complexation was also followed by UV spectrophotometric measurements. The formation of the [CdLH₂]⁴⁺ and [PbLH₃]⁵⁺ complexes at acidic pH values is accompanied by the appearance of a new red-shifted band at 334 nm, indicating the involvement of the terpyridine unit in metal coordination. Different from Cu(II) and Zn(II) coordination, this band does not show any significant change from acidic to strongly alkaline pH values, as shown in Figure 7 for Cd(II). Although the crystal structure of the {[CdLH]₂(µ-Br)}⁵⁺ assembly shows two monomeric Cd(II) complexes associated through a bridging bromide anion and π-stacking interactions, neither the potentiometric measurement nor the spectrophotometric measurement shows the formation of similar species in solution, even in the presence of added NaBr.

Compared to Zn(II) and Cu(II) complexation, the different coordination features of the Cd(II) and Pb(II) complexes in aqueous solution can be related to the softer and less acidic properties of these metal cations; this leads to a much lower affinity toward the hydroxide anion, consequently, to a lower tendency to form M₂(µ-OH) clusters.

The fluorescence emission of compound **L** is also strongly affected by metal coordination. Figure 8 reports the pH dependence of the fluorescence emission spectra recorded for solutions containing the ligand and Zn(II) in a 1:1 molar ratio. The comparisons of the fluorescence emission intensity of the ligand in the absence and in the presence of Zn(II) (Figure 8B) clearly show an increase in the fluorescence emission in the presence of the metal in the acidic pH region, where the [ZnLH₃]⁵⁺ complex is formed. Deprotonation of this complex to give the monoprotonated [ZnLH]³⁺ species, above pH 4.5, gives rise to quenching of the fluorescence emission. As in the case of the ligand alone, this behavior can be explained in terms of emission quenching through an electron-transfer process by amine groups not involved in proton or metal binding. It is well known, in fact, that Zn(II), like a proton, prevents fluorescence quenching through electron transfer involving the lone pair of an aliphatic amine group. Moreover, the quenching process by energy or electron transfer involving the metal is not efficient because of the d¹⁰ configuration of Zn(II). Most likely, in the [ZnLH₃]⁵⁺ complex, the aliphatic donors are involved
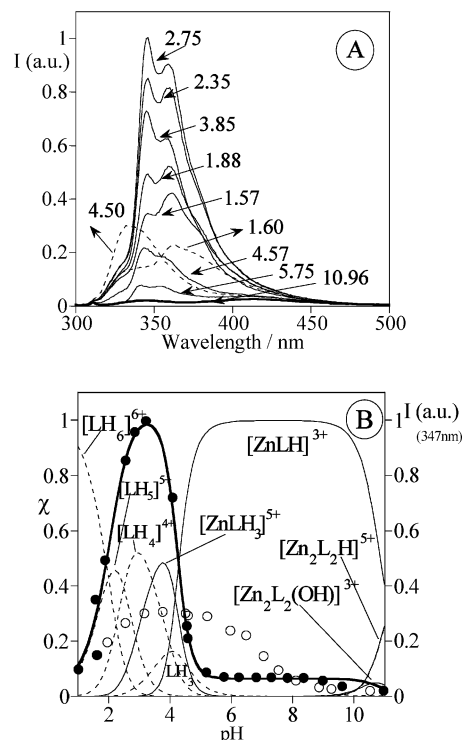

Figure 8. (A) Fluorescence emission spectra of the Zn(II) complexes with **L** at different pH values (excitation wavelength of 282 nm). (B) Fluorescence emission at 347 nm of **L** in the absence (○) and in the presence of Zn(II) (1:1 molar ratio) (●) and molar fractions of the protonated (- - -) and complexed species of **L** as a function of pH ([**L**] = 2.82 × 10⁻⁵ M; *I* = 0.1 M NMe₄Cl.).

either in metal coordination or in proton binding; therefore, their lone pairs are not available to quench the fluorescence emission. In the less protonated or unprotonated Zn(II) complexes, some amine groups do not participate in metal or proton binding, giving rise to the quenching process.

A similar behavior is also found in the case of Cd(II), where only the [CdLH₂]⁴⁺ complex is emissive. As often found in Cd(II) complexes, the emission intensity is less intense than in the case of Zn(II).[23a,44]

The profiles of the emission titration curves of free ligand **L** (Figure 2B) and its mononuclear Zn(II) complex (Figure 8B) show that both systems display fluorescence emission in a rather narrow pH window, that is, they behave as fluorescent sensors with an off/on/off response to pH.[45]

The fluorescence emission titration curves for the ligand alone and in the presence of Zn(II), Cd(II), Cu(II), and Pb(II) (1:1 metal-to-ligand molar ratio) are reported in Figure 9. Different from Zn(II) and Cd(II), in the case of Cu(II) and Pb(II), the fluorescence emission decreases upon metal binding, probably because of a possible energy-transfer process involving the metal.[46] The emission at acidic pH values observed in the case of Pb(II) is due to the presence of emissive protonated species of the free ligand. Different

(44) (a) Bazzicalupi, C.; Bencini, A.; Berni, E.; Bianchi, A.; Borsari, L.; Giorgi, C.; Valtancoli, B.; Lodeiro, C.; Lima, J. C.; Parola, A. J.; Pina, F. *J. Chem. Soc., Dalton Trans.* **2004**, 591−597. (b) Vicente, M.; Bastida, R.; Lodeiro, C.; Macías, A.; Parola, A. J.; Valencia, L.; Spey, S. E. *Inorg. Chem.* **2003**, *42*, 6768−6779.
(45) De Silva, A. P.; Gunaratne, H. Q. N.; McCoy, C. P. *Chem. Commun.* **1996**, 2399−2340.
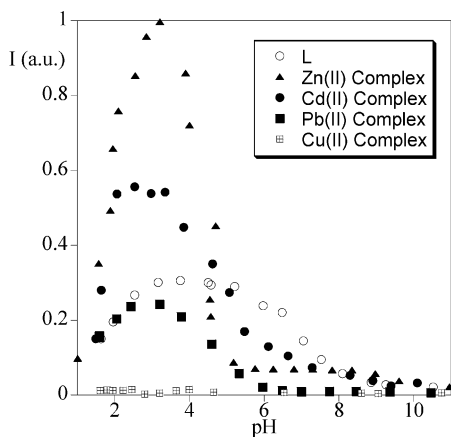
Figure 9. Fluorescence emission at 347 nm of **L** and its Pb(II), Zn(II), Cu(II), and Cd(II) complexes (1:1 molar ratio) as a function of pH ([**L**] = 2.82×10^{-5} M; $I = 0.1$ M NMe$_4$Cl).

Figure 10. UV−vis spectra recorded on aqueous solutions at pH 11 containing **L** and Zn^{2+} in different molar ratios: (*a*) 1:1, (*b*) 1:1.25, (*c*) 1:1.5, (*d*) 1:1.75, (*e*) 1:2, (*f*) 1:2.25, (*g*) 1:2.5 (0.1 mol dm^{-3} NMe$_4$Cl, T = 298.1 K).

from Cu(II) and Zn(II), in fact, Pb(II) is only partially complexed by **L** at acidic pH's, and a relevant number of protonated ligand species are present in solution.

As shown in Table 4, ligand **L** can also form dinuclear metal complexes with the metal under investigation. The addition of an increasing amount of Cu(II) or Zn(II) to solutions containing the dimeric complexes leads to a progressive red shift of the broad band at 310 nm and a simultaneous increase of the absorbance, to give, with a 2:1 metal-to-ligand molar ratio, the typical structured band at 335 nm of metal-coordinated terpyridine, as shown in Figure 10 in the case of Zn(II). These data account for the disruption of the dimeric species upon binding of a second Cu(II) or Zn(II) cation because of the increased electrostatic repulsion between two [M$_2$**L**]$^{4+}$ complexed units. In the case of Cd(II) and Pb(II), the addition of increasing amounts of the metals to the corresponding mononuclear complexes does not give any significant shift in the spectra. This suggests that in the dinuclear complex each metal is coordinated to a different binding moiety, the terpyridine unit and the polyamine chain, of the ligand.

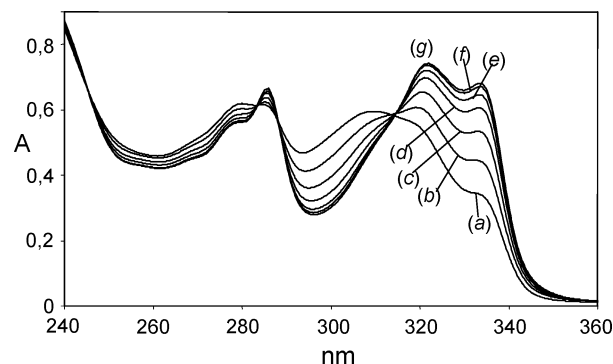Table 4 also shows that the dinuclear Cu(II), Zn(II), and Pb(II) complexes show a marked tendency to form hydroxo

complexes. In the case of Zn(II), the [Zn$_2$**L**(OH)]$^{3+}$ species is the only dinuclear complex formed in solution. Only in the case of Cd(II), no hydroxo complex is found; in this case, however, the system Cd/**L** in a 2:1 molar ratio was investigated only in the acidic pH region because of complex precipitation at alkaline pH values. The formation of stable dinuclear hydroxo species is generally attributed, in dinuclear complexes, to a bridging coordination of the hydroxide anion between two metal centers. Most likely, the two metals are kept at a close distance by the relatively small 24-membered cyclic framework, thus favoring the assembly of a Zn$_2(\mu$-OH) unit enclosed in the macrocyclic cavity.

Supporting Information Available: pH dependence of the absorption spectra of terpyridine in aqueous solution [L] = 1.95×10^{-5}. Speciation diagrams for the system **L**\Zn(II) at different concentrations. Plots of the ϵ values at 310 and 335 nm at pH 9.9 and 11.0 as a function of the overall percentage of the dimeric species. Crystallographic data in CIF format. This material is available free of charge via the Internet at http://pubs.acs.org.

IC049660L

(46) Alves, S.; Pina, F.; Albelda, M. T.; García-España, E.; Soriano, C.; Luis, S. V. *Eur. J. Inorg. Chem.* **2001**, *2*, 405−412. Czarnik, A. W. *Fluorescent Chemosensors for Ion and Molecule Recognition*; American Chemical Society: Washington, DC, 1993.